Comparative Analysis of Defect-Ground Type Electromagnetic Band-Gap Structures

#Ozgur Isik [1], Yuehe Ge[1], Karu P. Esselle [1]
[1]*Centre for Electromagnetic and Antenna Engineering, Department of Electronics, ICS Division, Macquarie University Sydney, NSW 2109, Australia, ozgur@ics.mq.edu.au*

Abstract

Planar electromagnetic band-gap (EBG) structures are considered to be very promising in microwave engineering and several designs have been proposed to improve band-gap performance. In this paper, the conventional defect-ground structures consisting of uniform or nonuniform periodic arrays of circles, complementary split ring resonators (CSRR) and recently proposed spiral electromagnetic band-gap (SEBG) structures are analyzed and compared. For circular-patterned EBGs, the center frequency of band-gap is determined by the array period, whereas in CSRR and SEBG structures the band-gap is mainly due to individual elements. This has been demonstrated by full-wave electromagnetic simulations. It is shown that SEBG structures are several times smaller than the others producing similar band-gap performance.

1. INTRODUCTION

Electromagnetic band-gap structures are periodic structures able to suppress the propagation of electromagnetic waves for specific frequency bands and directions [1]. Due to their unique properties, EBG structures have found various applications in the microwave domain including filters, antennas, power amplifiers and other microwave components [2]-[9]. In most applications, planar EBG structures are used due to their ease of manufacturing, low cost and integration compatibility with other circuits.

The conventional defect-ground type of planar EBG structures consist of a periodic uniform array of circles etched in a ground plane [3], [4]. Uniform distribution of the circular-patterned EBG structures gives rise to pass-band ripple which may be unacceptable for certain applications. With nonuniform circle dimensions, the pass-band ripple near the cut-off frequency can be suppressed. This is done by tapering the circle dimensions with certain distributions [5], [6]. Whether the dimensions are uniform or nonuniform, the conventional EBG structures are large in total length due to the need of many elements.

As an alternative, complementary split ring resonator (CSRR) was proposed for rejection of frequency bands [7], [8]. CSRR is obtained by replacing the concentric metallic rings of the original split ring resonator (SRR) with apertures, and vice versa. In this way, CSRRs can be etched in a ground plane. Although the band-gap property of CSRR is due to individual elements and not due to the array periodicity, it is still necessary to have many elements since the band-gap of the single element is very narrow.

Recently, we proposed spiral electromagnetic band-gap (SEBG) structures consisting of etched Archimedean spiral slots in a ground plane [9]. Similar to CSRRs, the band-gap is not determined by the periodicity but mainly by the element itself. SEBG structures have the advantages of wide band-gap, compact size, and many degrees of freedom to adjust the position of the stop-band. Furthermore, there is no pass-band ripple.

In this paper we present an analysis of above mentioned defect-ground type planar EBG structures with full-wave electromagnetic simulations and compare their band-gap performance along with overall physical dimensions.

2. DESIGN AND ANALYSIS

The transmission and reflection coefficients of a microstrip line over a defect-ground plane are used to analyze the structures. The defect-ground patterns are assumed to be etched in the metallic ground plane, which is on the bottom surface of a substrate. In all designs, the substrate has a thickness of 1.27 mm and a dielectric constant ε_r of 6.15. On the top surface, the microstrip line has a width of 1.9 mm and a characteristic impedance of $50\,\Omega$. Full-wave simulations have been conducted using Zeland IE3D 11.2.

We intend to achieve a 30% 20 dB stop-band width at the center frequency of 2.3 GHz.

A. Uniform Array of Circles

Fig. 1(a) shows the layout of a microstrip line with a uniform array of circular slots etched in the ground plane. According to the theory, the center frequency of stop-band is calculated approximately with the following equation [4]:

$$f_c \approx \frac{c}{2a\sqrt{\varepsilon_{eff}}} \qquad (1)$$

where c is the speed of light in free space, a is the array

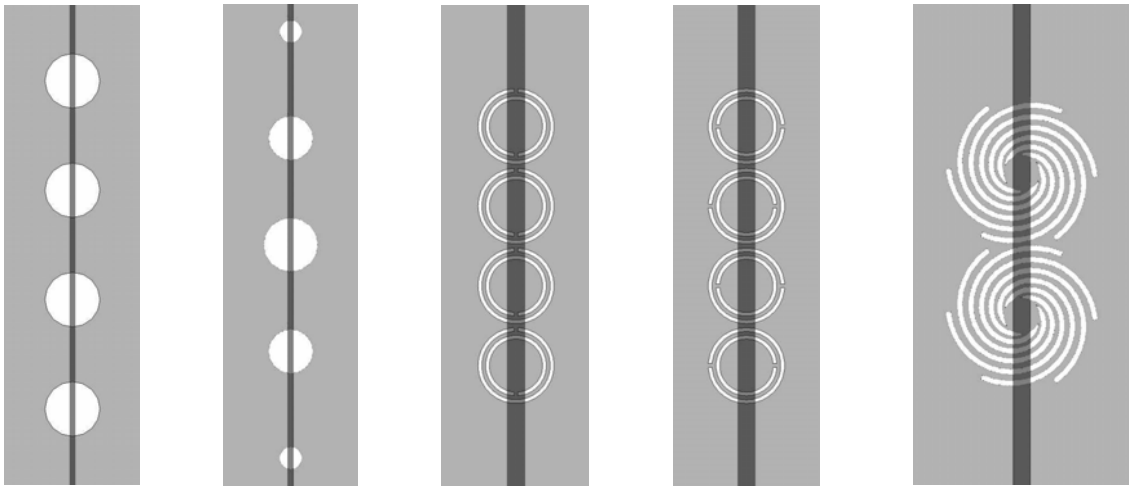

(a) (b) (c) (d) (e)

Fig. 1: Defect-ground type EBG structures: (a) Uniform array of circles. (b) Nonuniform array of circles. (c) CSRR of Type 1. (d) CSRR of Type 2. (e) Hexagonal SEBG.

period, which is the distance between the centers of two adjacent elements, and ε_{eff} is the effective dielectric constant of the substrate. After calculating from (1) and optimizing with full-wave analysis, we found the array period required for our stop-band as $a = 33.7$ mm. The structure was simulated for two different filling factors $r/a = 0.25$ ($r = 8.42$ mm) and $r/a = 0.375$ ($r = 12.63$ mm). The theoretical $|S_{21}|$ are plotted in dashed and solid lines in Fig. 2 for three and four unit cells, respectively. As can be seen in the figure, the higher the filling factor (*i.e*. circle radius), the higher the rejection amplitude and band-gap width, but also the more reinforced the amplitude of pass-band ripples. The performance figures and dimensions of the structures are presented in Table 1.

B. Nonuniform Array of Circles

To suppress the pass-band ripples near cut-off, different tapering techniques have been proposed to modify the dimensions of the circles [5], [6]. We studied two nonuniform distributions, namely binomial and Chebyshev, for circular slots as proposed in [6]. The coefficients of these polynomials are used to taper the circle dimensions resulting in a nonuniform structure, as shown in Fig. 1(b). The central element (or elements) is paired with the maximum amplitude of the coefficients and the rest of the elements follow the proportions. As in [6] we investigated two different relationships, the case when the coefficients are proportional to the radii of the circles and the case when the coefficients are proportional to the areas of the circles.

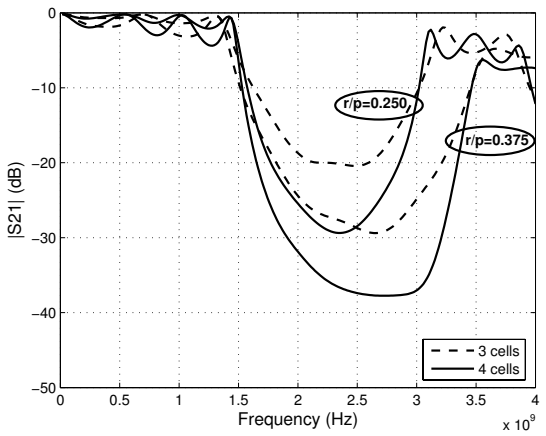

Fig. 2: $|S_{21}|$ versus frequency for uniform array of circular slots with different filling factors.

1) Binomial Distribution: In this section, the coefficients of binomial expansion [10], which are "1 2 1", "1 3 3 1", "1 4 6 4 1" and "1 5 10 10 5 1" for three, four, five and six elements array, respectively, have been used for tapering the circle dimensions. We first applied these to the radii and then to the areas of circular elements keeping the radius of the central circle(s) as $r_{\max} = 8.42$ mm. Here, the period is again 33.7 mm. Fig. 3 shows the theoretical $|S_{21}|$ in dashed lines for five cells and in solid lines for six cells. It is seen that the ripples near the cut-off frequencies have been suppressed remarkably, but at the expense of reduced rejection amplitude and consequently reduced band-gap width. The performance figures and dimensions of all four structures are given in Table 1. The rejection amplitudes are better for the case when the coefficients are proportional to the areas of the circles. However, in order to obtain a 20 dB band-gap width of 30%, more than five circular elements has to be used which increases the total length, greatly.

As a second approach we increased the radius of the central circle(s) to $r_{\max} = 12.63$ mm and reapplied the binomial distributions without changing the period. Simulation results are demonstrated in Fig. 4. As can be seen, the rejection amplitudes increased compared to the previous case, but with

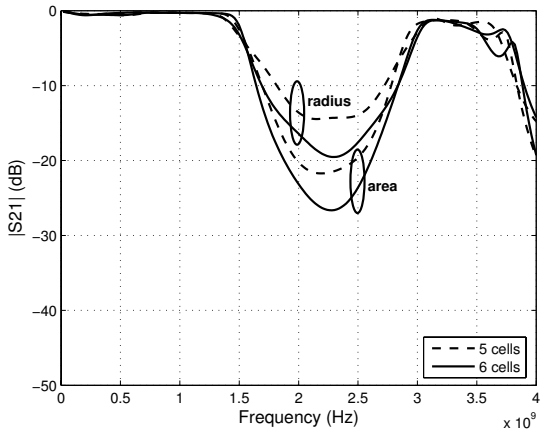

Fig. 3: $|S_{21}|$ versus frequency for nonuniform array of circular slots with binomial distribution of circle radii and areas (r_{max}=8.42 mm).

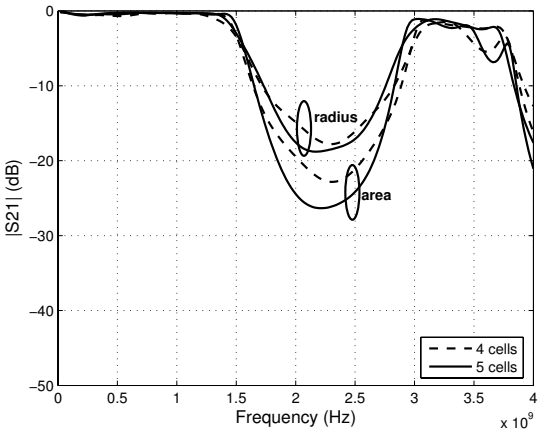

Fig. 5: $|S_{21}|$ versus frequency for nonuniform array of circular slots with Chebyshev distribution of circle radii and areas (r_{max}=8.42 mm).

some ripple in the pass-band. Table 1 summarizes the dimensions and performance figures.

2) Chebyshev Distribution: The coefficients of Chebyshev polynomial can be calculated by using the procedure given in [10]. For a voltage ratio of $R_0 = 30$ dB, the amplitudes are calculated as "0.429 1 1 0.429" for four elements array and "0.318 0.768 1 0.768 0.318" for five elements array. We applied Chebyshev distribution to the radii and areas of circular elements keeping the radius of the central circle(s) as $r_{\max} = 8.42$ mm. The array period was not changed. Fig. 5 shows the simulation results. It is seen that Chebyshev distribution produces slightly better performance than the binomial distribution with the same $r_{\max}$, and the length of overall structure is reduced. In order to obtain a 20 dB band-gap width of 30%, at least five circular elements are necessary. The details can be found in Table 1.

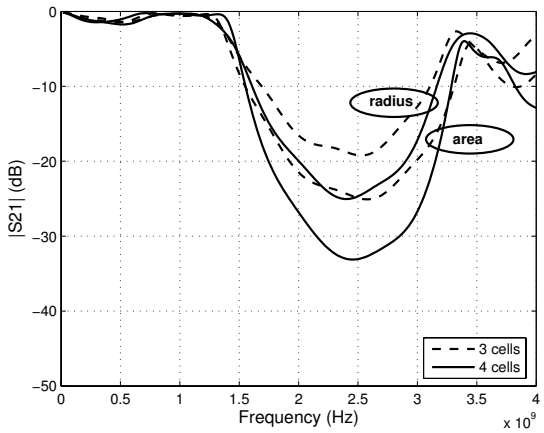

Fig. 4: $|S_{21}|$ versus frequency for nonuniform array of circular slots with binomial distribution of circle radii and areas (r_{max}=12.63 mm).

We also applied the Chebyshev distribution with $R_0 = 20$ dB and the circles with a maximum radius of 12.63 mm, but due to significant pass-band ripples, these designs were not taken into consideration.

C. Complementary Split Ring Resonator

Split ring resonators (SRR) are subwavelength magnetic resonant structures which are able to inhibit electromagnetic wave propagation in the vicinity of the resonant frequency, when excited by an axial magnetic field [7], [11]. A SRR consists of two concentric metallic rings with split on opposite sides and its resonance frequency can be tuned by varying the dimensions of the rings. Complimentary split ring resonators (CSRRs) are just the negative image of the SRRs and according to Babinet principle they exhibit characteristics which is almost dual of that of the SRRs [7]. So CSRRs are able to provide a stop-band around the resonance frequency when excited by an axial electric field. It is important to note that the stop-band achieved is not due to Bragg-like diffraction, but to the behavior of constituent elements [7], [8]. Therefore, the array period can be very small, which then reduces the overall dimensions compared to conventional EBG structures.

Fig. 1(c) shows the layout of a microstrip line with CSRR structures etched in the ground plane. As can be seen, in *Type 1*, the splits of all elements are placed in the same direction, towards the microstrip line port. In order to investigate the influence of the position of the splits, we simulated several cases by rotating each unit cell by 90° intervals. The widest stop-band has been obtained when the splits of the consecutive unit cells are placed in opposition to each other and in a direction orthogonal to the microstrip line, as shown in Fig. 1(d). We call this *Type 2*. In both cases, the radius of the outer ring is 4 mm, the radius of the inner ring is 3.2 mm, the distance between the rings is 0.4 mm, the ring width is 0.4 mm, and the slit width is 0.4 mm. The array period is 8.4 mm

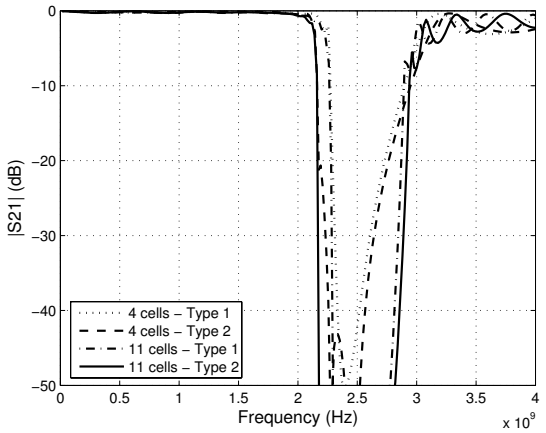

Fig. 6: $|S_{21}|$ versus frequency for four and eleven unit cells of CSRR of Type 1 and Type 2.

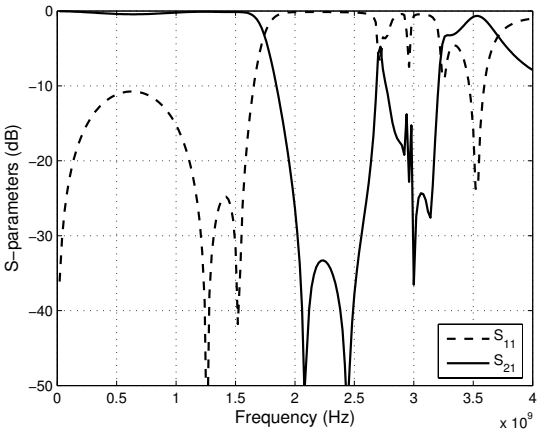

Fig. 8: Simulated S-parameters versus frequency for two unit cells of hexafilar SEBG structure with disconnected spiral arms.

and the substrate is the same as before.

Fig. 6 shows the theoretical $|S_{21}|$ of both cases for four and eleven unit cells. According to the figure, CSRRs can provide deep rejection band with very sharp cut-offs along with no pass-band ripple. However, the stop-band of a single unit cell is very narrow. Therefore, in order to obtain a 20 dB band-gap width of 30%, at least eleven Type 2 elements has to be used which results in a total length of 90 mm. The performance figures and dimensions of all four CSRRs are given in Table 1.

Another issue that has to be considered when dealing with this type of resonant structures is the radiation loss. The loss factor is calculated as $LF = 1 - |S_{11}|^2 - |S_{21}|^2$ and plotted in Fig. 7 for the CSRR structures discussed above. In the figure, resonant peaks are observed at around both the lower and higher cut-off frequencies. As the substrate and the metal layers are assumed to be lossless, this rise in the loss factor is due to strong radiation, which is a result of the resonant behavior of the structure, and can be undesirable in some applications.

D. Spiral EBG Structures

Recently, we proposed Archimedean spiral electromagnetic band-gap (SEBG) structures as a very compact geometry of producing high rejection band [9]. These new structures consist of a number of Archimedean spirals, also known as logarithmic spirals, etched in a ground plane. SEBG structure provides many degrees of freedom to adjust the stop-band position for close-fit designs. Similar to CSRR, SEBG structure exhibits relatively sharp cut-offs and a flat pass-band. The band rejection property is mainly due to individual cells, not due to the array periodicity; the cut-off frequency depends on the arc length of the spiral arm. Therefore, only a couple of unit cells of SEBGs are sufficient in order to

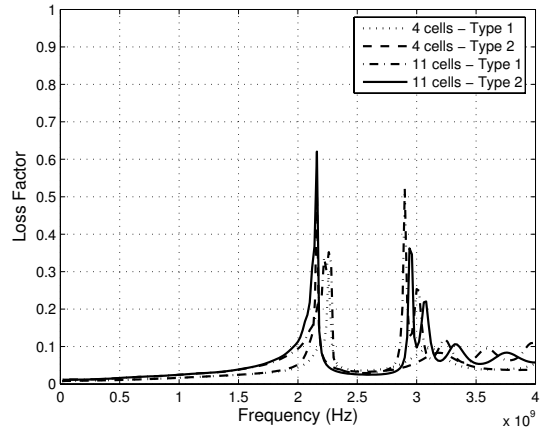

Fig. 7: The loss factor versus frequency for four and eleven unit cells of CSRR of Type 1 and Type 2.

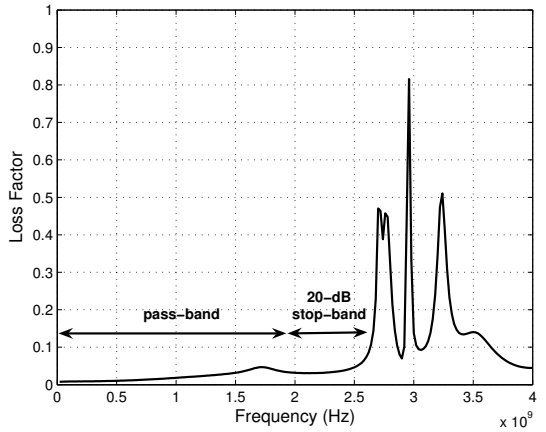

Fig. 9: The loss factor versus frequency for two unit cells of hexafilar SEBG structure with disconnected spiral arms.

TABLE 1: COMPARATIVE STUDY OF DEFECT-GROUND TYPE EBG STRUCTURES

Class	Type		Number of Cells	Pass-band Ripple	Max Band Rejection (dB)	20 dB Stop-band Width (%)	Total Length (mm)
Uniform Array of Circles	r/p=0.250		3	High	20	18	84.2
			4	High	29	47	117.9
	r/p=0.375		3	High	29	56	92.7
			4	High	38	68	129.4
Binomial Array of Circles	r_{max}=8.42 mm	radius, r	5	No	14	0	137.6
			6	No	19	0	170.2
		area, πr^2	5	No	22	22	141.7
			6	No	27	33	178.8
	r_{max}=12.63 mm	radius, r	3	Moderate	19	0	80.0
			4	Moderate	25	36	109.5
		area, πr^2	3	Moderate	25	43	85.3
			4	Moderate	33	57	115.7
Chebyshev Array of Circles	r_{max}=8.42 mm	radius, r	4	No	18	0	108.3
			5	No	19	0	140.2
		area, πr^2	4	No	23	23	112.1
			5	No	26	30	144.3
CSRR	Type 1		4	No	50	18	33.2
			11	No	62	23	92.0
	Type 2		4	No	68	24	33.2
			11	No	61	30	92.0
SEBG	Hexagonal		2	No	54	30	30.9

achieve a wide band-gap. Design procedure and formulas for cut-off frequency calculation are given in [9].

Here, we take hexafilar SEBG with disconnected arms as an example. As shown in Fig. 1(e), the hexafilar spiral geometry is realized by combining six spiral arms with a rotation of 60° relative to each other. The polar equation of the first spiral is given by

$$r = A\theta^{1/n}, \quad 0 \le \theta \le \phi \quad (2) \qquad (2)$$

where ϕ is the sweep angle of the spiral; A and n are constants. The six spiral slots are disconnected from each other by imposing a small metal circle (with radius r) in the center. The structure analyzed has the following parameters: $n = 0.7$, $A = 0.35$, $\phi = 2.85\pi$ rad, $r = 2$ mm, and *slot width*=0.5 mm. The array period is 16 mm and the substrate is the same as before.

Theoretical S-parameters for two unit cells of this structure are plotted in Fig. 8. It is clear that only two unit cells of hexafilar SEBG can provide the targeted 20 dB band-gap width of 30%. Furthermore, the loss due to radiation is very low, *i.e.* less than 10%, within both the pass-band and stop-band regions as illustrated in Fig. 9. As presented in Table 1, the total length of the SEBG structure is 30.97 mm which is almost three times shorter than that of its nearest competitor, *i.e.* CSRR - Type 2.

3. CONCLUSION

A comparative study of the conventional circular EBG structures (with uniform and nonuniform distributions) CSRRs and SEBG structures has been presented. The band-gap and pass-band characteristics along with physical dimensions of the structures have been determined and compared using IE3D simulations.

Conventional uniform arrays of circular slots are able to produce a stop-band due to periodicity, but they suffer from pass-band ripples. By modifying the circle dimensions according to binomial and Chebyshev distributions, the pass-band ripples have been significantly suppressed, but at the expense of reduced band-gap width, reduced rejection amplitude and increased total physical length. Unlike conventional EBG structures, CSRRs can produce a stop-band due to their resonant behavior. Although they provide relatively deep rejection bands along with no pass-band ripple, it is seen that the stop-band of one element is very narrow. This has been improved by placing the splits of consecutive cells in opposition to each other as in CSRR Type 2.

SEBG structures are very compact and efficient way of obtaining band-gap property. Similar to CSRRs, they exhibit resonant behavior but their radiation loss is low in both stop-band and pass-band. More importantly, only two unit cells of the hexafilar SEBG structure with disconnected spiral arms is sufficient to achieve a 20 dB stop-band width of 30%. The total physical length of SEBG structure is three to six times shorter than the other structures that produce a 30% stop-band.

REFERENCES

[1] J. D. Joannopoulos, R. D. Meade, and J. N. Winn, *Photonic Crystals: Molding the Flow of Light*, Princeton, NJ: Princeton University Press, 1995.

[2] C. Caloz and T. Itoh, *Electromagnetic Metamaterials: Transmission Line Theory and Microwave Applications*, Hoboken, NJ: John Wiley & Sons, 2006.

[3] V. Radisic, Y. Qian, R. Coccioli, and T. Itoh, "Novel 2-D photonic bandgap structure for microstrip lines," *IEEE Microwave Guided Wave Lett*., vol. 8, no.2, pp. 69–71, Feb. 1998.

[4] C. C. Chiau, X. Chen, and C. Parini, "Multiperiod EBG structure for wide stop-band circuits", *IEE Proc.-Microw. Antennas and Propagat.*, vol. 150, No. 6, pp. 489-492, Dec. 2003.

[5] M. A. G. Laso, T. Lopetegi, M. J. Erro, D. Benito, M. J. Garde, and M. Sorolla, "Novel wideband photonic bandgap microstrip structures," *Microwave Opt. Tech. Lett.*, vol. 24, no. 5, pp. 357–360, Mar. 2000.

[6] N. C. Karmakar and M. N. Mollah, "Investigations Into Nonuniform Photonic-Bandgap Microstripline Low-Pass Filters," *IEEE Trans. Microwave Theory Tech*., vol.51, pp.564-572, Feb. 2003.

[7] F. Falcone, T. Lopetegi, J.D. Baena, R. Marqués, F. Martin, and M. Sorolla, "Effective Negative-ε Stop-band Microstrip Lines Based on Complementary Split Ring Resonators", *IEEE Microwave and Wireless Comp. Lett.*, vol.14, pp. 280-282, June 2004.

[8] X. Ying and A. Alphones, "Propagation characteristics of complimentary split ring resonator (CSRR) based EBG structure," *Microwave Opt. Tech. Lett*., vol. 47, no. 5, pp. 409-412, Dec. 2005.

[9] O. Isik, Y. Ge, and K. P. Esselle, "Novel Spiral EBG Structures," *12th International Symposium on Antenna Technology and Applied Electromagnetics (ANTEM),* Montreal, Canada, pp. 561-564, 2006.

[10] C. A. Balanis, *Antenna Theory Analysis and Design*, pp. 243-249, NY: Harper & Row, 1982.

[11] J. B. Pendry, A. J. Holden, D. J. Robbins, and W. J. Stewart, "Magnetism from conductors and enhanced nonlinear phenomena," *IEEE Trans. Microwave Theory Tech.*, vol. 47, pp. 2075–2084, Nov. 1999.